INTER-CALIBRATION OF ERS AMI AND METOP ASCAT BACKSCATTER MEASUREMENTS

Christoph Reimer [(1)], Sebastian Hahn [(1)], Wolfgang Wagner [(1)]

[(1)] Vienna University of Technology
Department of Geodesy and Geoinformation
Research Group Remote Sensing

christoph.reimer@geo.tuwien.ac.at
sebastian.hahn@geo.tuwien.ac.at
wolfgang.wagner@geo.tuwien.ac.at

ABSTRACT

Scatterometer derived products have become an important input dataset for climate change research. For this reason accurate radiometric calibration of scatterometer is a prime requirement from the scientific community to enable them to establish a long-term consistent scatterometer dataset. The calibration method that we introduce here is a stepwise relative calibration approach using extended area Land-Targets. Intra-calibration of a scatterometer mission will account for instrument related drifts, while inter-calibration is performed to identify possible difference of various scatterometer missions. Similarities in instrument design of ERS-2 AMI and MetOp-A ASCAT allow the merging of these datasets, with the proposed stepwise calibration approach, and result in global backscatter observations spanning over 20 years.

1 INTRODUCTION

With the launch of the European Remote Sensing satellite (ERS-1) in July 1991, the first European C-Band scatterometer was placed in orbit to gather information from the Earth's surface in the microwave spectrum. Subsequently three further European scatterometers were launched on-board ERS-2 and the Meteorological Operational satellites (MetOp) - A/B, providing continuous radar backscatter measurements of the Earth's surface.

Scatterometers are real aperture radars designed to make accurate measurements of the radar cross section, sigma nought (σ^0), sacrificing range and spatial resolution. The original aim of spaceborne scatterometer was to observe wind speed and direction over the oceans, but applications over land also emerged, monitoring cryosphere, vegetation and soil surface properties. Derived scatterometer products, so called Level 2 or Level 3 products [1], such as surface soil moisture [2] or surface wind fields [3], became an important input dataset for climate change research. Hence, scatterometers have to be well calibrated during their mission lifetime and across different missions to meet the challenge of capturing climate changes from space.

The Active Microwave Instrument (AMI), operating in wind mode, onboard ERS-1 and ERS-2 is a C-Band fan-beam scatterometer with three sideways looking vertically polarised antennas, one looking perpendicular to the right side of the satellite track (Mid-Beam), one looking forward at 45° angle (Fore-Beam) and one looking backward at 135° angle (Aft-Beam) illuminating a 500 km wide swath [4]. The instrument technical design of the Advanced Scatterometer (ASCAT) onboard MetOp-A/B is similar to AMI but with an enhanced system geometry of six fan-beam antennas illuminating two swaths separated from the satellite ground track by about 336 km [5]. A sun-synchronous polar orbit was chosen for both satellites with descending and ascending equator crossing times at approximately 10:30 and 22:30 local mean time respectively. Similarities in the instrument technical design of AMI and ASCAT facilitate the fusion of these datasets to a homogenous time series comprising more than 20 years of backscatter measurements for climate change research. Therefore a precise radiometric calibration of these instruments is required. In the case of scatterometers, two types of radiometric calibration methods can be distinguished: internal and external calibration. Internal calibration is used to monitor variations in the transmitter and receiver chain of the instrument and is performed directly onboard [4], [6].

To estimate the total end-to-end performance of the instrument, it is crucial to perform external calibration. Targets with a well-known signal response are used to determine the relationship of transmitted and measured signal affected by the antenna. Two strategies of external calibration of spaceborne scatterometer are commonly used. Using active transponders, acting as Point-Targets with a well-established radar cross section, allow deducing calibration information about the antenna pattern across the main lobe [7]. Calibration performed with transponders assesses absolute calibration errors in the radar cross section by

Proc. 'ESA Living Planet Symposium 2013', Edinburgh, UK
9–13 September 2013 (ESA SP-722, December 2013)

computing the difference of returned and transmitted signal of the target. Since calibration information using transponders is sampled at distinct position in the antenna pattern, a second approach for antenna pattern fine tuning was proposed based upon extended area Land-Targets [8]. Targets of this type are characterised by stable radar cross section signature over an extensive area. This calibration approach is often referred to as relative calibration, published in several studies concentrating on different targets and calibration models [9]–[12]. In this paper a relative stepwise radiometric calibration approach using extended areas land-targets is proposed. To account for backscatter inconsistencies during a specific scatterometer mission, sensor "intra-calibration" is introduced. The objective of sensor "inter-calibration" is to identify and correct for possible variations between various scatterometer missions. A few studies are published examining scatterometer inter-calibration [11], [13], [14], [12]. In these studies inter-calibration methods can be categorised into model-based and backscatter-collocation procedures. While inter-calibration relying upon backscatter-collocation requires simultaneous backscatter observations of scatterometer missions, this requirement can be relaxed in model-based methods using extended area Land-Targets.

Datasets under investigation are Level 1 backscatter measurements obtained from ERS-2 AMI (May 1997 to February 2003) and MetOp-A ASCAT (January 2007 to December 2012). The spatial resolution of both datasets is about 25 km with both providing an almost global spatial coverage. To derive backscatter time series for analysis both datasets were resampled from swath observation geometry to an earth-fixed global grid, with a spacing of 12.5 km.

2 CALIBRATION METHODOLOGY

Calibration errors cause inconsistencies in radar backscatter measurements and degrade the accuracy of higher level scatterometer products. The stepwise calibration approach will account for inconsistencies in ERS-2 AMI and MetOp-A ASCAT mission separately and between these two missions. Extended area land-targets with a well-defined radar backscatter response are selected to estimate intra- and inter-calibration coefficients. To account for sensor specific variations the coefficients are applied globally to the raw Level 1 backscatter measurements. The subsequent subsections discuss the selection of suitable extended area land-targets for calibration, estimation of sensor intra-calibration coefficients and the inter-calibration approach in detail.

2.1 Selection of extended area Land-Targets

Investigations relating to the characterisation and location of suitable calibration targets have been undertaken since the early stages of space scatterometry [15]–[17], [9], [18]. Characteristics of extended area land-targets for radiometric calibration of spaceborne scatterometers can be summariesed as follows.

- σ^0 should be known at radar frequency, polarisation and incidence angle of interest.
- dependency of σ^0 on azimuth angle should be small and well understood
- Calibration target with large spatial extent
- Spatial variations of σ^0 within the target should be small and well understood
- σ^0 dependency on the time of the year should be known
- σ^0 dependency on the time of the day should be known
- Target conditions should remain constant during the missions

Consequently a calibration target must indicate an azimuthal isotropic, temporal stable and spatial homogenous backscatter response. These calibration target characteristics are examined via global statistics of Level 1 backscatter measurements normalised to an incidence angle of θ=40° by a linear model. Global statistics of the mean normalised backscatter $\overline{\sigma^0}(40°)$,

$$\overline{\sigma^0}(40°) = \sum_{i=1}^{N} \overline{\sigma^0}(40°, \varphi_i) \qquad (1)$$

the temporal stability ν

$$\nu = \sqrt{\sum_{i=1}^{N} \left(\sigma^0(40°, \varphi_i) - \overline{\sigma^0}(40°, \varphi_i)\right)^2} \qquad (2)$$

and azimuthal anisotropy δ of the normalised backscatter are carried out to select calibration targets by creating spatial masks generated by applying thresholds to these parameters.

$$\begin{gathered} \delta_A = |\sigma^0{}_F(\varphi_1) - \sigma^0{}_A(\varphi_3)| \\ \delta_D = |\sigma^0{}_F(\varphi_1) - \sigma^0{}_A(\varphi_3)| \\ \delta = \max(\delta_A, \delta_D) \end{gathered} \qquad (3)$$

The thresholds for these parameters are chosen to be minimal compared to the global average. Two suitable calibration targets are found with this method, namely Amazon Rainforest (pink) and Congo Rainforest (orange) for both scatterometer datasets (Fig. 1). In-homogenous backscatter values within the extended area land-targets regions, such as rivers or urban areas, are successfully masked out.

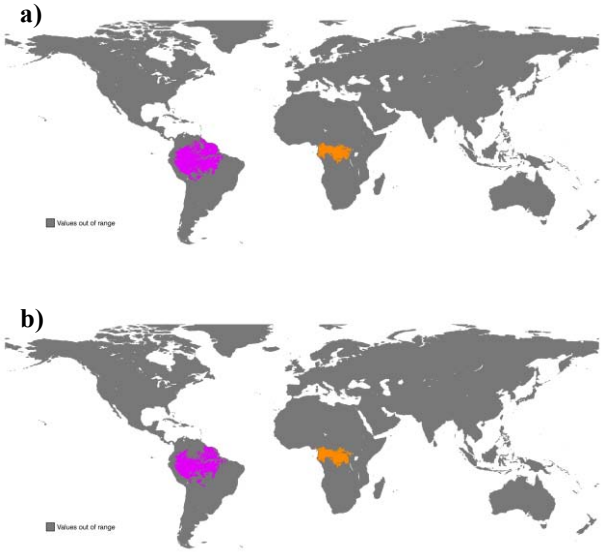

Figure 1: Extended area Land-Targets selected with threshold approach, a) ERS-2 AMI b) MetOp-A ASCAT

2.2 Sensor Intra-Calibration

In general the radar backscatter response of a target is a function of location (L), time (t), incidence (θ) and azimuth (φ) angle. The proposed backscatter measurement model (Eq. 4) is composed of the true radar cross section $\widehat{\sigma^0}(L, t, \theta, \varphi)$, the gain error $G_E(t, \theta, \varphi)$ and noise ε.

$$\sigma^0(L, t, \theta, \varphi) = \widehat{\sigma^0}(L, t, \theta, \varphi) + G_E(t, \theta, \varphi) + \varepsilon \qquad (4)$$

When considering extended area Land-Targets, exhibiting no spatial, temporal or azimuthal dependency on the radar backscatter, the measurement model can be simplified to Eq. 5.

$$\sigma^0(t, \theta, \varphi) = \widehat{\sigma^0}(\theta) + G_E(t, \theta, \varphi) + \varepsilon \qquad (5)$$

Moreover the true radar cross section ($\widehat{\sigma^0}$) becomes a function of the incidence angle exclusively and Eq. 5 can be solved for $G_E(t, \theta, \varphi)$, to determine gain error estimates.

$$G_E(t, \theta, \varphi) + \varepsilon = \sigma^0(t, \theta, \varphi) - \widehat{\sigma^0}(\theta) \qquad (6)$$

A so called reference model is used to estimate the unknown true radar cross section $\widehat{\sigma^0}(\theta)$ for each calibration target separately to infer gain error estimates for intra-calibration. Therefore the gain error of each calibration target is initially supposed to be $G_E(t, \theta, \varphi) = 0$. A second order polynomial was fitted to the data of each calibration target, with respect to the incidence angle θ, representing the mean backscatter behaviour of the target. Additionally, separate models are derived for ascending and descending overpasses.

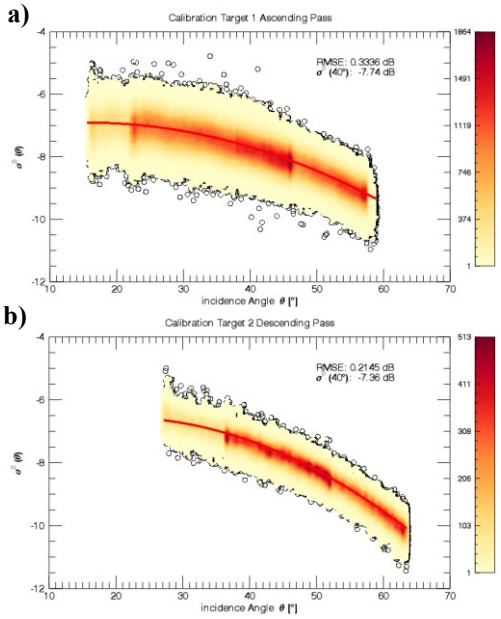

Figure 2: Reference Models (red line) of a) ERS-2 AMI Amazon Rainforest ascending overpass b) MetOp-A ASCAT Congo Rainforest descending overpass

With these reference models and Eq. 6, estimates of the gain error $G_E(t, \theta, \varphi)$ are calculated. Assuming a linear relationship between the gain error $G_E(t, \theta, \varphi)$ and the incidence angle θ, a gain error model $\widehat{G}_E(t, \theta, \varphi)$ is calculated for each azimuth angle per month, as an average of the n calibration targets.

$$\widehat{G}_E(t, \theta, \varphi) = \frac{1}{n}\sum_{i=1}^{n} \overline{G_E}(t, 40°, \varphi) + A_G(t, \theta - 40°, \varphi) \qquad (7)$$

Finally, intra-calibration coefficients can be calculated based on the gain error model $\widehat{G}_E(t, \theta, \varphi)$, to perform sensor intra-calibration by subtracting the coefficient from the measurement (Eq. 8).

$$\sigma^0{}_{cal}(L, t, \theta, \varphi) = \sigma^0(L, t, \theta, \varphi) - \hat{G}_E(t, \theta, \varphi) \qquad (8)$$

2.3 Sensor Inter-Calibration

Inter-calibration of AMI and ASCAT can be done after sensor intra-calibration. The measurement model after intra-calibration for each sensor is given in Eq. 9.

$$\sigma^0{}_{ASCAT}(\theta) = \widehat{\sigma^0{}_{ASCAT}}(\theta) + \varepsilon_{ASCAT}$$
$$\sigma^0{}_{AMI}(\theta) = \widehat{\sigma^0{}_{AMI}}(\theta) + \varepsilon_{AMI} \qquad (9)$$

To inter-calibrate AMI against ASCAT, estimates of the inter-calibration error are determined by Eq. 10.

$$G_C(\theta, i) = \widehat{\sigma^0{}_{ASCAT}}(\theta) - \sigma^0{}_{AMI}(\theta, i) \qquad (10)$$

The error estimates are further used to set up a linear inter-calibration error model with respect to the incidence angle. The linear model is deduced as an average over all n targets for each scatterometer beam (i) and centred at an incidence angle of θ=40°.

$$\widehat{G}_C(\theta, i) = \frac{1}{n}\sum_{j=1}^{n} \overline{G_C}(40°, i) + A_C(\theta - 40°, i) \qquad (11)$$

3 Results

The first results of this calibration method are provided in this section of the paper. The monthly evolution of $\sigma^0(40°)$ of ERS-2 AMI in ascending overpass for Amazon Rainforest is given in Fig. 3. Deviations of $\sigma^0(40°)$ to the reference model are related to gain errors during the mission. The Aft-Beam antenna of ERS-2 AMI in particular, shows a strong increase in backscatter after May 2001 compared to the reference model. These gain errors after May 2001 can be removed from the Level 1 backscatter measurements by applying sensor intra-calibration. The evolution of the calibrated data indicates a successful gain error removal, exhibiting smaller deviations of each beam compared to the reference model and an almost stable backscatter response.

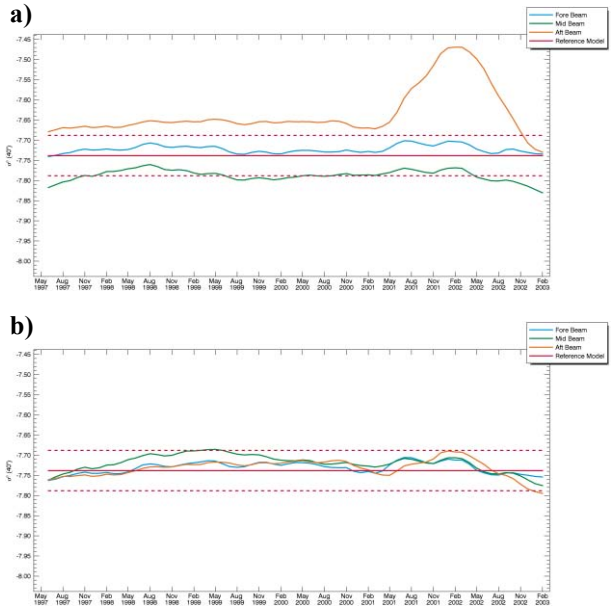

Figure 3: Sensor Intra-Calibration ERS-2 AMI ascending overpass for Amazon Rainforest
a) un-calibrated b) calibrated

Monitoring of the gain error of MetOp-A ASCAT indicates an intra-calibration error of the Mid-Beam antenna in the left swath of the instrument in July 2009. The origin of this gain error is unknown but clearly visible in the monitoring. Furthermore, the implementation of a new calibration table to the ground processor at EUMETSAT in August 2011 causes inconsistencies in the backscatter measurements of the mission. As a result of this ground processor update, the backscatter response decreases by approximately 0.1 dB, but all these mission related effects can be accurately remove performing sensor intra-calibration.

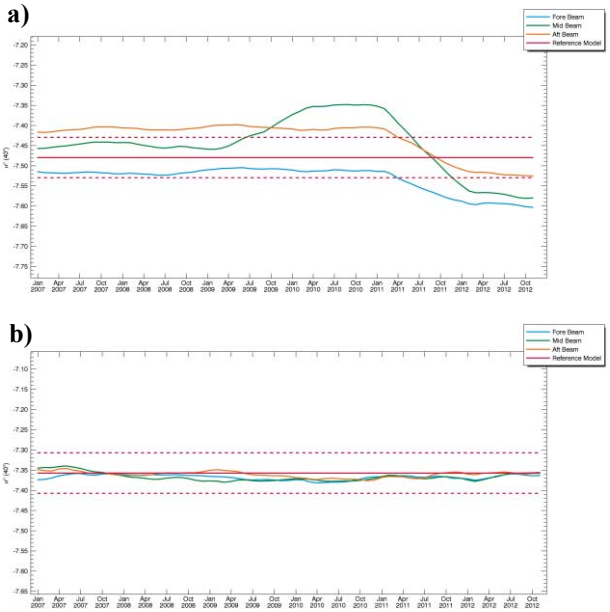

Figure 4: Sensor Intra-Calibration MetOp-A ASCAT descending overpass for Congo Rainforest
a) un-calibrated b) calibrated

The linear inter-calibration model of AMI and ASCAT is sufficient to describe differences between these instruments as can be seen in Fig. 5-7. Inter-calibration results of AMI and ASCAT are very similar for each antenna. The mean bias between the two instruments is about 0.13 dB for ascending and 0.11 dB for descending overpasses at an incidence angle of θ=40.

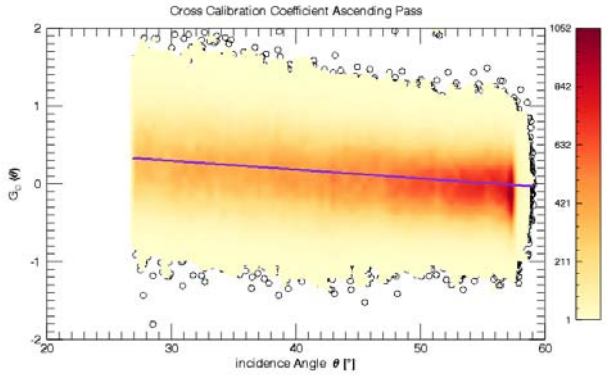

Figure 5: Aft-Beam ascending overpass inter-calibration model (violet line) and estimates of inter-calibration error as density-scatterplot

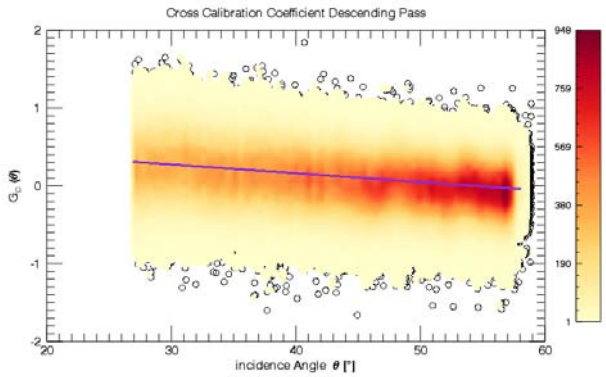

Figure 6: Fore-Beam descending overpass inter-calibration model (violet line) and estimates of inter-calibration error as density-scatterplot

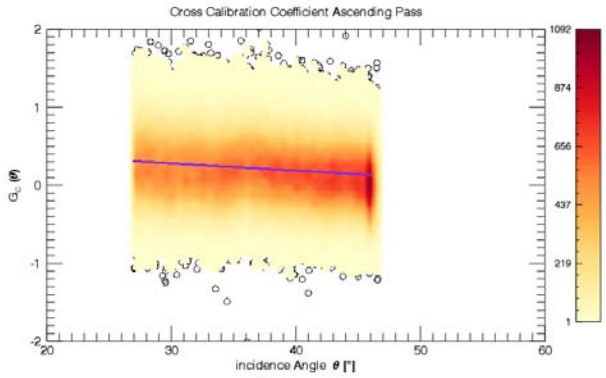

Figure 7: Mid-Beam ascending overpass inter-calibration model (violet line) and estimates of inter-calibration error as density-scatterplot

4 CONCLUSION

Long-term Level 2 or Level 3 scatterometer derived products have become a crucial input dataset for climate change research. Hence an accurate radiometric calibration of these datasets is required to meet the scientific challenges. The proposed stepwise radiometric calibration approach accounts for variations during a specific scatterometer mission and across various missions. Intra-calibration of ERS-2 AMI and MetOp-A ASCAT show that instrument related drifts, such as electronic component aging, antenna deformation or ground processor changes can be correctly removed. Differences in the radar backscatter response of AMI and ASCAT are modelled during inter-calibration of these two scatterometer mission, indicating a bias of 0.13 dB for ascending and 0.11 dB for descending overpasses respectively. Considering instrument related drifts and biases between ERS-2 AMI and MetOp-A ASCAT will result in a consistent dataset of global backscatter measurements, comprising more than 20 years of data for climate change research.

5 REFERENCES

[1] V. Bennett and S. James, "Guidelines for Data Producers - Climate Change Initiative Phase 1," Technical Note CCI-PRGM-EOPS-TN-11-0003, May 2013.

[2] W. Wagner, G. Lemoine, and H. Rott, "A Method for Estimating Soil Moisture from ERS Scatterometer and Soil Data," *Remote Sensing of Environment*, vol. 70, no. 2, pp. 191–207, Nov. 1999.

[3] A. Stoffelen, "Scatterometry," University of Utrecht, Utrecht, 1998.

[4] E. P. W. Attema, "The Active Microwave Instrument on-board the ERS-1 satellite," *Proceedings of the IEEE*, vol. 79, no. 6, pp. 791 – 799, Jun. 1991.

[5] J. Figa-Saldaña, J. J. W. Wilson, E. Attema, R. Gelsthorpe, M. R. Drinkwater, and A. Stoffelen, "The advanced scatterometer (ASCAT) on the meteorological operational (MetOp) platform: A follow on for European wind scatterometers," *Canadian Journal of Remote Sensing*, vol. 28, no. 3, pp. 404–412, Jun. 2002.

[6] P. Lecomte, "ERS scatterometer instrument and the on-ground processing of its data," in *European Space Agency, (Special Publication) ESA SP*, 1998, pp. 241–260.

[7] C. Anderson, H. Bonekamp, J. Wilson, J. Figa, A. de Smet, and C. Duff, "CALIBRATION AND VALIDATION OF ASCAT BACKSCATTER," 2011.

[8] P. Lecomte and W. Wagner, "ERS Wind Scatterometer Commissioning & In-Flight Calibration," *EUROPEAN SPACE AGENCY-PUBLICATIONS-ESA SP*, vol. 424, pp. 261–270, 1998.

[9] D. G. Long and G. B. Skouson, "Calibration of spaceborne scatterometers using tropical rain forests," *IEEE Transactions on Geoscience and Remote Sensing*, vol. 34, no. 2, pp. 413–424, Mar. 1996.

[10] L. B. Kunz and D. G. Long, "Calibrating SeaWinds and QuikSCAT Scatterometers Using Natural Land Targets," *IEEE Geoscience and Remote Sensing Letters*, vol. 2, pp. 182–186, Apr. 2005.

[11] Z. Bartalis, "ERS-ASCAT Backscatter and Soil Moisture Intercomparison - First Results.," Institute of Photogrammetry and Remote Sensing, Vienna University of Technology, Vienna, Working Note 6, 2009.

[12] A. Elyouncha and X. Neyt, "C-Band Satellite Scatterometer Intercalibration," *IEEE Transactions on Geoscience and Remote Sensing*, vol. 51, no. 3, pp. 1478–1491, Mar. 2013.

[13] A. Elyouncha, X. Neyt, and M. Acheroy, "Radiometric cross-calibration of spaceborne

scatterometers-first results," in *Proceedings of SPIE - The International Society for Optical Engineering*, Berlin, 2009, vol. 7473.

[14] M. Talone, R. Crapolicchio, G. De Chiara, X. Neyt, A. Elyouncha, L. S. De Miguel, G. Davies, and B. Bojkov, "Cross-calibration of ERS-1 and ERS-2 wind scatterometers; Towards a homogeneous 20-year-long wind vector monitoring of the earth," 2012, pp. 4606–4609.

[15] I. J. Birrer, E. M. Bracalente, G. J. Dome, J. Sweet, and G. Berthold, "Sigma-0 Signature of the Amazon Rain Forest Obtained from the Seasat Scatterometer," *IEEE Transactions on Geoscience and Remote Sensing*, vol. 20, no. 1, pp. 11–17, Jan. 1982.

[16] R. G. Kennett and F. K. Li, "Seasat over-land scatterometer data. I. Global overview of the Ku-band backscatterer coefficients," *Geoscience and Remote Sensing, IEEE Transactions on*, vol. 27, no. 5, pp. 592–605, 1989.

[17] R. G. Kennett and F. Li, "Seasat over-land scatterometer data. II. Selection of extended area and land-target sites for the calibration of spaceborne scatterometers," *Geoscience and Remote Sensing, IEEE Transactions on*, vol. 27, no. 6, pp. 779–788, 1989.

[18] P. L. Frison and E. Mougin, "Use of ERS-1 wind scatterometer data over land surfaces," *Geoscience and Remote Sensing, IEEE Transactions on*, vol. 34, no. 2, pp. 550–560, 1996.